Understanding the role of cloud microphysical processes behind the Indian summer monsoon rainfall

Ushnanshu Dutta[1,2] · Anupam Hazra[1] · Hemantkumar S. Chaudhari[1] · Subodh Kumar Saha[1] · Samir Pokhrel[1]

Abstract

Cloud microphysical processes and rainfall over the Indian summer monsoon (ISM) region are unique because of the strong interaction among clouds, thermodynamics, and dynamics. The heating and presence of water vapor during ISM help for the formation of cloud particles in stratiform and convective clouds. In this study, we have analyzed the role of cloud microphysical processes behind the ISM rainfall (ISMR) and their inter-annual and sub-seasonal variability from the Goddard Earth Observing System (GEOS) model data (i.e., MERRA reanalysis). The spatial distribution of microphysical process rates (e.g., auto-conversion, freezing, accretion of rain and snow) over the Indian subcontinent are in line with the rainfall distribution. Besides, the interannual variability of these cloud microphysical process rates is coupled to that of the ISMR. It is revealed that these microphysical processes are in line with the spatial distribution of more (less) rainfall over the Indian subcontinent during active (break) spells. They also have significant sub-seasonal variability like ISMR over the ISM region. The variance is more in the synoptic scale than in quasi-biweekly mode (QBM) and monsoon intraseasonal oscillation (MISO) scales. Further, the sub-seasonal variances of microphysical process rates are well correlated with the mean ISMR. Results also reveal the teleconnection of cloud microphysical processes over the ISM region with the ENSO phenomena. We hope that the understanding of detailed microphysical processes during ISM will help the development of a climate model for depicting the mean monsoon. It may then enhance the skill of seasonal prediction.

1 Introduction

The Indian summer monsoon (ISM) rainfall (ISMR) is one of the most important large-scale phenomena, driven by ocean–atmosphere interaction (Meehl 1989; Nobre and Shukla 1996; Trenberth et al. 2000; Zhou et al. 2008). It acts as a pivotal water source for the countries of the Indian subcontinent. It is not only the lifeline of the people residing but also the impetus of the gross domestic product (GDP) of these countries (Gadgil and Gadgil 2006; Parthasarathy et al. 1988). Hence, policymakers are interested in the prediction of this variability well advanced for disaster management and crop management.

Why is understanding the detailed microphysical process rates important? Cloud and its propagation are important for

monsoon (Sikka and Gadgil 1980), and cloud microphysics in particular, which includes microphysical processes (viz. autoconversion, accretion, freezing, and evaporation), is crucial in seasonal and intraseasonal scales (Hazra et al. 2016, 2017a, b; Dutta et al. 2020, 2021). Kumar et al. (2017) have pointed out that, a better understanding of various multi-scale processes which drive the MISOs is the key to achieving better fidelity in coupled climate models. The parameterizations of condensation, freezing, sublimation, evaporation, autoconversion, accretion, and sedimentation of liquid and ice (Bacmeister et al. 2006) are important for sustaining monsoon dynamics through latent heating and rainfall formation (Tao et al. 1990, 2001; Hazra et al. 2016). Therefore, understanding the detailed microphysical process rates may help to target the improvement of the particular processes in a climate model.

Though the understanding of these detailed cloud microphysical processes for ISM precipitating clouds is important to fix the target (i.e., tendency equations) in the model code for developing coupled climate models, the studies in this direction over the ISM region are limited. Wonsick et al. (2009) have performed a detailed analysis of cloud amounts

✉ Anupam Hazra
  hazra@tropmet.res.in

1 Ministry of Earth Sciences, Indian Institute of Tropical Meteorology, Pune, India 411008

2 Department of Atmospheric and Space Sciences, Savitribai Phule Pune University, Pune, India

and their occurrence using satellite data over different locations, during different phases of monsoon. Chakravarty et al. (2018) from radar observation found that the transition phase from break spell to active is due to the increase of the congestus clouds. Our earlier studies (Hazra et al. 2017a,b, 2020a, b; Dutta et al. 2020, 2021, 2022) demonstrated that proper representation of cloud microphysical processes in climate models can improve the simulation of mean and intraseasonal features of ISMR through the dynamical and thermodynamical structure of ISM.

On the other hand, despite significant improvements in modeling resources and computation facilities, the skill score of coupled global climate models (CGCMs) is far below the potential predictability (PP) limit (Krishna Kumar et al. 2005; Rajeevan et al. 2012). Can the improved understanding of cloud microphysical processes improve this? Kulkarni et al. (2011) found that the predictability of the seasonal mean depends on the credibility of the prediction of MISOs. Limitations in prediction skills can be arising from the unrealistic parameterization of cloud processes and precipitation physics in climate models (Kumar et al. 2017; Hazra et al. 2017a, b; Dutta et al. 2020). Hence, De et al. (2019) highlighted the need for more research on the interaction between cloud and large-scale circulation process which they found a "gray area in climate science." Tiwari et al. (2014) found that these low skill scores may originate from sparse representation of observed teleconnection of ISMR with Pacific SST, i.e., El-Nino and Southern Oscillation (ENSO), revealed in numerous studies (Krishnamurthy and Goswami 2000; Ropelewski and Halpert 1989; Sikka 1980; Mooley and Parthasarathy 1984; Pradhan et al. 2016; Goswami and Xavier 2005; Goswami and Jayavelu 2001; Pokhrel et al. 2012; Dwivedi et al. 2015). In general, these studies highlight that moderate to strong El-Nino-like conditions are responsible for below-normal monsoon to deficient (droughts) conditions. Besides, several studies (Burns et al. 2003; Srivastava et al. 2002; Chang et al. 2001; Chattopadhyay et al. 2015; Sankar et al. 2016; Borah et al. 2020) have discussed the role of other non-ENSO predictors (viz., North Atlantic Oscillations (NAO), Atlantic Multidecadal Oscillations (AMO), and Extra Tropics (ET) in regulating the ISMR. Recently, Saha et al. (2019) observed that synoptic components of the ISMR are also potentially predictable which uplifts the potential predictability (PP) limit. In subsequent works (Saha et al. 2019, 2020, 2021) they argued that ISMR has a high predictability and the simulation of sub-seasonal statistics, particularly the synoptic systems, hold the key for skillful prediction on seasonal to decadal time scale. The synoptic system is primarily governed by lows and depressions that form over the Bay of Bengal and travels west and north-westward (Saha et al. 2020; Godbole 1977; Stowasser et al. 2009; Revadekar et al. 2016; Krishnamurthy and Ajayamohan 2010; Hurley and Boos 2015).

Several studies (Sarker and Choudhary 1988; Prasad et al. 1990; Stano et al. 2002; Hunt et al. 2016) have performed a composite analysis of different variables, taking a different number of LPS. Recently, Hazra et al. (2020b) discussed the fidelity of different cloud microphysical parameterization schemes to simulate the characteristics of LPS which traverse from the Bay of Bengal to the Indian mainland and have an intensity of deep depressions using the Weather Research and Forecasting (WRF) model. However, none of these studies discussed the cloud microphysical processes in the LPS.

Upon surveying the literatures, we found a lack of studies that discuss cloud microphysical processes in interannual, sub-seasonal scales (i.e., synoptic, QBM, and MISO) as well as for LPS. Hence, in this endeavor, we have addressed the following:

i)   Role of cloud microphysical process in governing the seasonal mean rainfall and its interannual variability.
ii) Possible linkage of microphysical processes with ENSO.
iii) Cloud microphysical processes in synoptic (3–7 days), quasi-biweekly mode (QBM: 10–20 days), and MISO (30–60 days) scales.
iv) Linkage between ISMR and cloud microphysical processes in the sub-seasonal (synoptic, QBM and MISO) scales.
v)   Composite analysis of the cloud processes of LPS that passes through Central India.

2 Data and methodology

These analyses are based on Modern Era Retrospective-analysis for Research and Applications—version 2 (MERRA2, Gelaro et al. 2017) reanalysis data. The MERRA2 replaced its predecessor MERRA, which was terminated on March 2016. MERRA2 is based on the Goddard Earth Observing System (GEOS) atmospheric data assimilation system version 5.12.4. It contains GEOS atmospheric model (Rienecker et al. 2008; Molod et al. 2015) and the Gridpoint Statistical Interpolation (GSI) analysis scheme (Wu et al. 2002; Kleist et al. 2009). The model includes the finite-volume dynamical core of Putman and Lin (2007), and has an approximate resolution of $0.5° × 0.625°$ and 72 pressure levels from the surface to 0.01 hPa. A detailed description of the MERRA2 product can be found in the Gelaro et al. (2017) study. The GEOS model included using the Earth System Modeling Framework (ESMF) (Rienecker et al. 2008), where the cloud scheme in the GEOS model considers a single phase of condensate. The cloud microphysics for cloud water and ice/snow is taken care of explicitly, as presented by Bacmeister et al. (2006) and Barahona et al. (2014). It is to

be noted that MERRA2 data used here are data assimilation products that consume observations and should not be deemed proper observations. Bao and Zhang (2019) also used MERRA data for their study over the Tibetan Plateau region. The same data is also used for the study of tropical cyclones (Jones et al. 2021) and tropical tropopause breaks (Luan et al. 2020).

The cloud microphysical tendency terms taken from MERRA2 data are autoconversion of cloud water to rain (RAUT), accretion of cloud water to rain (RACR), accretion of cloud water to snow (SACR), and net freezing of cloud condensate into ice (FCI). The daily and monthly rainfall data are taken from Global Precipitation Climatology Product (GPCP; Adler et al. 2003). These data are in the range 1980–2019 except for daily rainfall data from GPCP, which is in the range 1997–2019. LPS dates are taken from Regional Meteorological Centre Chennai (RMCC), under India Meteorological Department (IMD) (http://www.imdchennai.gov.in/) during the period 1980–2019 for June to September (JJAS) season only. It provides the tracks of all depressions, cyclones, and severe cyclonic storms since 1891 forming over the Bay of Bengal, Land, and the Arabian Sea. The LPS which traverse through the central India region $(72 - 88° \, E, \, 18 - 28° \, N)$ are only considered irrespective of intensity in this study. Marginal no of LPS found that forms over the Arabian Sea and traverse through CI. Hence, they are not considered here. The composites of LPS events are made on the basis of dates on which the LPS (forming over the Bay of Bengal and Land) are over land region only. The sea surface temperature (SST) data sets used in the study are obtained from Hadley center global sea Ice and Sea Surface Temperature (HadiSST; Rayner et al. 2003).

The cloud microphysical processes, which include cloud water and ice in both convective and grid-scale parameterizations, are important for the parameterization of surface precipitation.

In the simple cloud scheme, the predictive model equations for cloud water/ice mixing ratio q_c can be written as:

$$\frac{\partial q_c}{\partial t} = -Advection + TurbulentTerm + C_{\text{cov},grid-scale} - E_{c,r} - P$$

where the first two terms are advection and turbulent terms. Condensation (convective and grid-scale) is denoted as $C_{\text{conv,gridscale}}$. The term $E_{c,r}$ is the evaporation of cloud and rain and P denotes precipitation. Condensation, auto-conversion, accretion, and deposition are key processes for the formation of rain (Zhao & Carr 1997; Grabowski 1998).

$$P = AUT + ACR + AGG$$

where AUT is the "autoconversion," and ACR and AGG are accretion and aggregation terms respectively.

$$ACR = RACR + SACR$$

where RACR and SACR are the rain accretion and snow accretion respectively.

The cloud scheme in the Goddard Earth Observing System (GEOS) model considers a single phase of condensate. The microphysical processes such as autoconversion, evaporation/sublimation, and accretion of cloud water and ice/snow are taken care of explicitly as presented by Bacmeister et al. (2006). The relaxed Arakawa–Schubert (RAS, Moorthi and Suarez 1992) is used for moist convection parameterization. All types of freezing (homogeneous, heterogeneous, e.g., immersion, contact), which are important for the formation of cloud ice, are treated in the GEOS model (Barahona et al. 2014). The collection of cloud ice to snow and the graupel or aggregation process depend on the primary source of cloud ice, which is coming from the "freezing" process. The JJAS mean climatology of auto-conversion accretion and freezing of cloud ice are highly correlated with ISM mean rainfall (Hazra et al. 2016). Therefore, we are devoting this study to the understanding of the important microphysical processes (e.g., autoconversion, freezing, accretion of rain and snow) for the ISM clouds and precipitation.

The normal monsoon years (NY), excess (formerly flood) years (EY), deficient (formerly drought) years (DY), and El-Nino/La-Nina years are obtained from "Monsoon On Line" site maintained by the Indian Institute of Tropical Meteorology, Pune, India (https://mol.tropmet.res.in/). The interannual deviation of rainfall during $1980 - 2019$ is shown in Figure S1. The sub-seasonal oscillations in different bands, i.e., Synoptic, QBM, and MISO, of concerned variables were calculated by applying the Lanczos band-pass filter of $2 - 7$ days, 10–20 days, and 30–60 days respectively. Active-Break dates are taken from our earlier study (Dutta et al. 2020). Outgoing longwave radiation (OLR) data are taken from the National Oceanic and Atmospheric Administration (NOAA) (Liebmann and Smith 1996). Specific humidity, high cloud fraction, and wind data are taken from the fifth generation of the European Centre for Medium-Range Weather Forecasts (ECMWF) reanalysis, ERA5 (Hersbach et al. 2020) for the period of $1980 - 2019$.

The coefficient of variation (CV, Hendricks and Robey 1936) is calculated as

$$\text{Coefficient of variation} = \frac{\text{standard deviation}}{\text{mean value}}$$

3 Results and discussions

3.1 Descriptions of the cloud microphysical processes

We have considered four important microphysical processes, namely (i) rain auto-conversion (RAUT), (ii) rain accretion

(RACR), (iii) snow accretion (SACR), and (iv) freezing of cloud ice (FCI). The RAUT conversion is controlled by a parameterization that follows Kessler (1969) such that the rate at which cloud water is converted to rainwater is given by:

$$\left(\frac{\partial q_r}{\partial t}\right)_{auto} = A(q_c - q_0)$$

where q_c is the cloud liquid water mixing ratio and $A = 10^{-3} \, s^{-1}$ represents the rate at which the conversion takes place when $q_c > q_0$.

Autoconversion is the initial stage of the collision–coalescence process, in which bigger droplets with more fall velocity collect smaller ones and form embryonic rain drops (Liu et al. 2004, 2005; Cheng et al. 2007). Hence, it acts as a primary source of rainwater in precipitation (Hazra et al. 2015, 2016) followed by the collision growth process which is termed accretion. Rain accretion (RACR) is the collection of cloud drops by larger rain drops while falling through a cloud, which depends on both cloud and rainwater mixing ratios (q_c and q_r) (Kessler 1969). The conversion terms of precipitation, due to the accretion of cloud droplets by snow is called snow accretion (SACR), while autoconversion is responsible for precipitation initiation, accretion controls the intensity of precipitation (Wu et al. 2018). Snow accretion plays a crucial role in the cold rain processes (Pruppacher and Klett 1997) as it is related to the melting (Hazra et al. 2013) of mixed-phase hydrometeors (snow and graupel). The cold rain process plays a pivotal role in simulating the seasonal (Hazra et al. 2016) and intraseasonal features (Dutta et al. 2020) of ISM in coupled climate models.

The process involved in ice particle formation is called freezing of cloud ice (FCI). The ice crystal nucleation by homogeneous and heterogeneous freezing is controlled by temperature and supersaturation. The highest supersaturation values correspond to low temperatures with high vertical velocities (Barahona et al. 2014). Now, the formation of cloud ice due to the freezing of cloud water (Mason 1971) in the atmosphere acts as a primary source of snow and graupel. The freezing process also acts as the controlling factor for cloud ice to snow autoconversion and collection of cloud ice by snow. Now, the autoconversion and accretion of rain depend on the cloud water mixing ratio (Kessler 1969; Tripoli and Cotton 1980; Khairoutdinov and Kogan 2000; Wood 2005). Autoconversion of cloud ice to snow (Hazra et al. 2016; Zhao et al. 2017) is also an important microphysical process which is responsible for the formation of snow and subsequent increment of it (snow) by accretion of snow (Yamasaki 2013). Therefore, the formation of deep convection is related to the formation of more FCI and then SACR.

3.2 Interannual variability of cloud microphysical processes

Firstly, it is important to compare the JJAS mean climatology of rainfall of the GEOS model (product of MERRA2) with observation (GPCP) before looking into the results of microphysical process rates from MERRA2. Figure 1 demonstrates the 40 years of JJAS climatology of rainfall from observation (GPCP) and MERRA2 reanalysis (which is the product of the GEOS model), along with the microphysical processes. The rainfall climatology is consistent between GPCP and MERRA2 quantitatively and qualitatively over the South Asian Monsoon region as well as the ISM region (PCC ~ 0.9). The consistency of the MERRA2 rainfall annual cycle (Hazra et al. 2016) and spatial pattern studies (Hamal et al. 2020; Reichle et al. 2017) with observation provide the confidence to study the role of detailed microphysical process rates (which can be available only from the model product) on the formation of rainfall. The maxima of rainfall over ISM are noticed over the Western Ghats, northeast India, extending to the Bay of Bengal (BoB). A considerable amount of rainfall is received over the central India region and Himalayan foothills as well. The climatology of microphysical processes is well associated with the spatial distribution of rainfall climatology over the whole basin. Maxima of freezing of cloud condensate are noticed over the Bay of Bengal. Maxima of ice-water content are also reported (Rajeevan et al. 2013) over this region from satellite data. The rain auto-conversion (RAUT, ~ 6.4 mm/day) is the most among the microphysical processes over the ISM region (70–90° E, 10–30° N), followed by rain accretion (RACR, ~ 2 mm/day), snow accretion (SACR, ~ 1.5 mm/day), and freezing of cloud ice (FCI, ~ 0.3 mm/day). Moderate to high values of PCC of different microphysical processes over ISM give a quantitative estimate of their association with mean rainfall (Observation ~ 7.5 mm/day, MERRA2 ~ 7 mm/day). The PCC is higher in RACR (~ 0.7), followed by RAUT (~ 0.6), SACR (~ 0.5), and FCI (~ 0.3).

It is revealed that cloud microphysical process rates are highly modulating rainfall formations. Therefore, the question arises: Is there any role of these processes on the interannual variation of the mean rainfall? To get a quantitative estimate, we have computed the temporal (40 years) correlation of these processes with the mean rainfall averaged over the ISM region. All of these processes show a high ($r > 0.5$) and significant correlation (above 95%) with the mean rainfall. The RAUT and RACR show a similar correlation ($r \sim 0.8$). The correlation is a little less in the case of SACR and FCI ($r \sim 0.6$). Increment (decrement) of rainfall over the Indian land region is noticed in EY (DY), which is consistent with the similar variation in the microphysical processes (Fig. S2, S3). There is a significant difference (Fig. 2) in these processes (e.g., RAUT, RACR, SACR, and

Fig. 1 JJAS climatology of rainfall from **a** GPCP and **b** MERRA2. **c** Autoconversion of cloud water to rain (RAUT), **d** accretion of cloud water to rain (RACR), **e** accretion of cloud water to snow (SACR), and **f** freezing of cloud condensate into ice (FCI). ISM region (70–90° E, 10–30° N) averaged value of respective variables are written at the top left corner. Pattern correlation of the microphysical processes with the mean rainfall over the ISM region is also given in parenthesis. Period: 1980–2019. Unit: mm/day
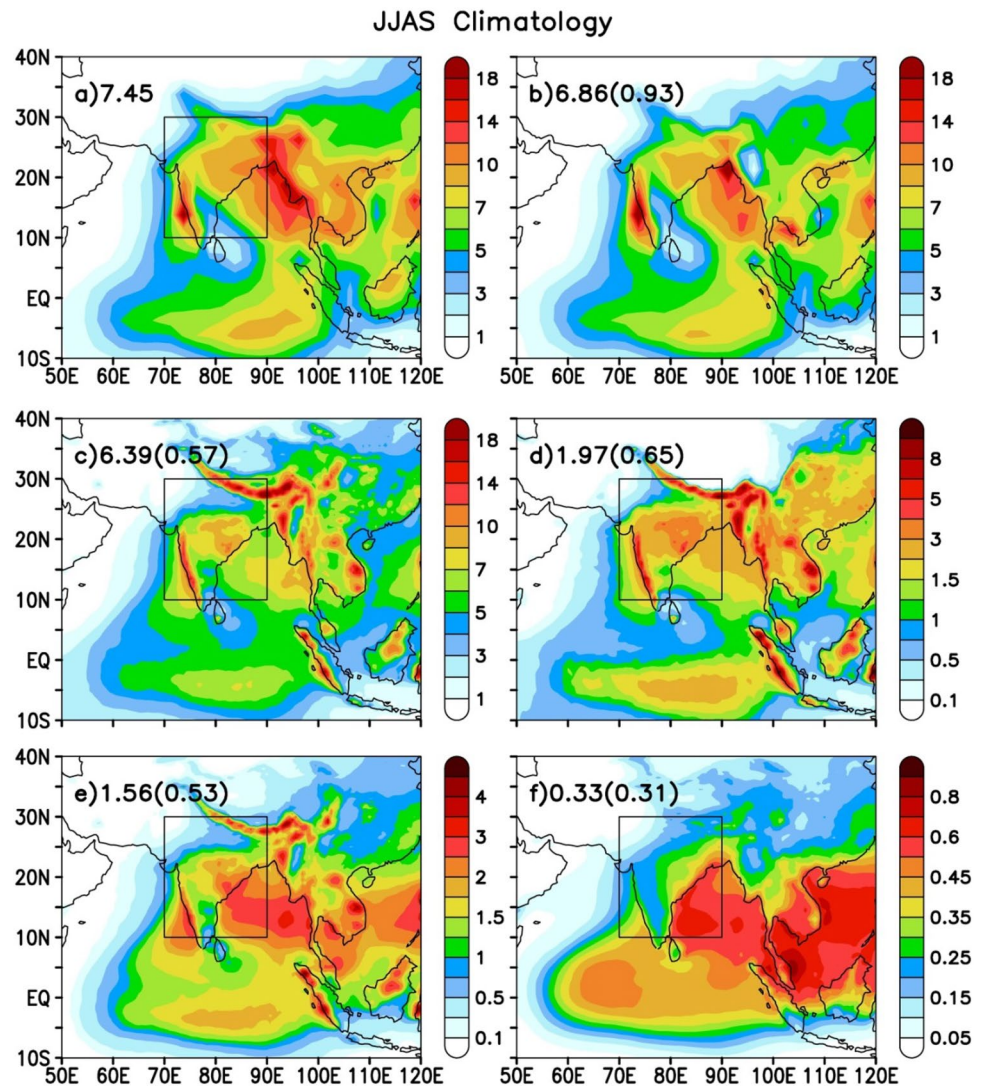
FCI) over the Indian land and adjacent oceanic regions (BoB and the Arabian Sea), which manifest in the formation of rainfall. The difference between EY and DY clearly unveils that, all of these processes and thus rainfall are stronger over the ISM region during above normal years as compared to below normal years (Fig. 2, Fig. S2, S3). To understand the influence of ENSO on microphysical processes, which are key elements for rain formation, we have further bifurcated the deficient years into two parts, i.e., El-Nino plus deficient years (EDY) and non-El-Nino plus deficient years (NEDY). Decrement of rain and associated microphysical processes (Fig. 3) are found to be more in EDY (Fig. S4) as compared to NEDY (Fig. S5).

In a quantitative estimate, we have computed the percentage deviation of these composites from the climatological values over central India's homogeneous monsoon region (72 − 88° E, 18 − 28° N, Fig. 4). Results show increment (decrement) in rain percentage (∼ 10%) during EY (DY) over this region. During EDY, the rainfall decreases in higher

percentage than NEDY. All the microphysical processes are enhanced during EY as compared to DY. These processes are more declined in EDY than NEDY (Fig. 4).

3.3 Sub-seasonal variability of cloud microphysical process

It is important to note that the seasonal mean summer monsoon rainfall is coming from the combined contributions of vigorous sub-seasonal oscillations (i.e., active and break spells) (Goswami 2005) and synoptic disturbances (e.g., lows, depression, etc.). The monsoon intraseasonal oscillation (MISO), which is dominated by 30–60-day and 10–20-day modes in the temporal domain, represents vigorous fluctuations. Wang et al. (2005) showed that a coupled global climate model (CGCM) is essential for a reliable forecast of mean monsoon on the sub-seasonal time scale. Most of the CGCMs participating in the Coupled Model Intercomparison Project-Phase 5 and 6 (CMIP5, CMIP6) have dry rainfall

Fig. 2 Difference between the composite of excess years (EY) and deficient years (DY) of rainfall from GPCP (**a**) and cloud microphysical processes i.e. RAUT (**b**), RACR (**c**), SACR (**d**), and FCI (**e**) from MERRA2
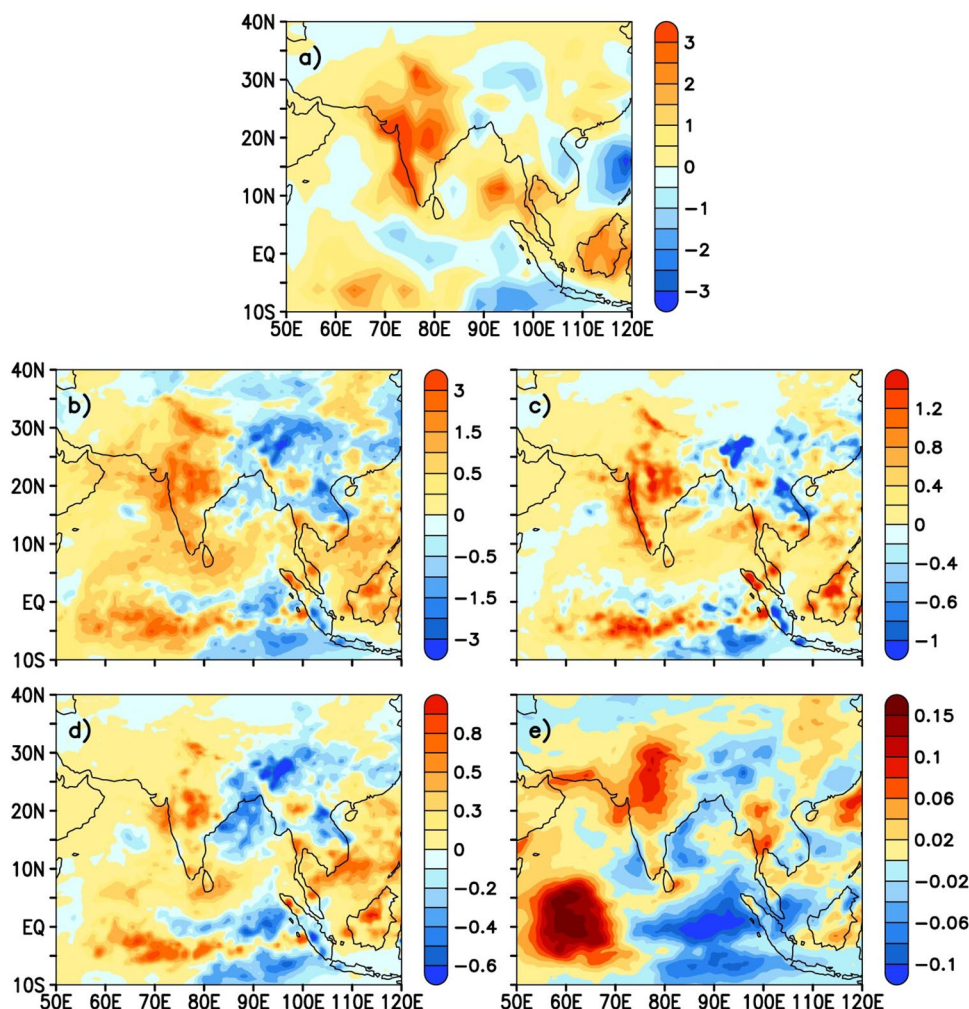
bias (Goswami & Goswami 2017; Choudhury et al. 2021; Dutta et al. 2022). The underestimation of rainfall in most of the CGCMs may be linked with the bifurcation of two types of rain (stratiform and convective), which again linked with the vertical structure of diabatic heating and the dry bias propagation of the 30–60-day mode (Kumar et al. 2017; Goswami & Goswami 2017; Dutta et al. 2021). Therefore, here, we have discussed the microphysical processes rates from MERRA2 data and rainfall from GPCP in active to break spells. The active and break periods (dates) are taken from the earlier study of Dutta et al. (2020). Figure 5 shows the difference between active and break composite of rainfall and microphysical process (RAUT, RACR, SACR, and FCI) anomalies. More (less) rainfall is observed over the Indian landmass (equatorial Indian Ocean) during active spells as compared to break spells. Quantitatively, the difference in rainfall between active and break composite over ISM (averaged) is approximately 9 mm/day. All the microphysical processes behave like rainfall distribution highlighting their important roles in active/break spells. The difference in RAUT is the highest (~4 mm/day), followed by RACR

(~2 mm/day), SACR (~1 mm/day), and FCI (~0.1 mm/day). The high pattern correlations over the south Asian monsoon region (50–120° E, 10° S–40° N) of these processes ($r \sim 0.8$ for RAUT, RACR, and SACR and $r \sim 0.6$ for FCI) with rainfall, for the difference between active and break spells, reveals the significance and association of these processes with spatial variation of rainfall quantitatively. These findings are consistent with an earlier study by Hazra et al. (2016).

Goswami et al. (2003) put forward a hypothesis that the increase (decrease) in rainfall over the monsoon trough region during active (break) spells is attributed to the modulation of the genesis of synoptic-scale low-pressure systems (i.e., lows and depressions, etc.) through modulation of the large-scale monsoon flow (Krishnamurthy and Ajayamohan 2010; Praveen et al. 2015). Several studies (Stowasser et al. 2009; Revadekar et al. 2016; Krishnamurthy and Ajayamohan 2010; Hurley and Boos 2015) found that majority of these low-pressure systems (LPS) develop in the Bay of Bengal, with typical time scales of 3–5 days. Of these LPS, on average, approximately 14 are reported to occur each

Fig. 3 Same as Fig. 2 but for the difference between the composite of El-Nino + deficient years (EDY) and non-El-Nino + deficient years (NEDY)
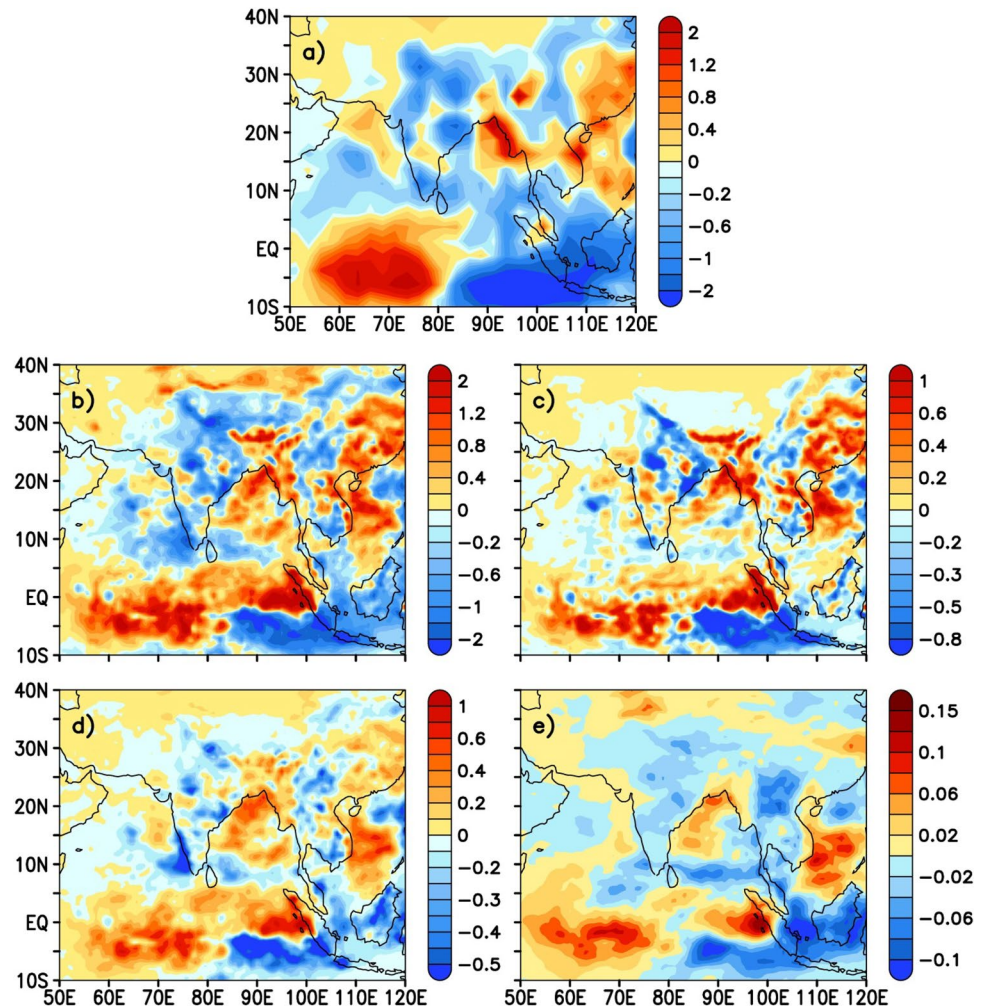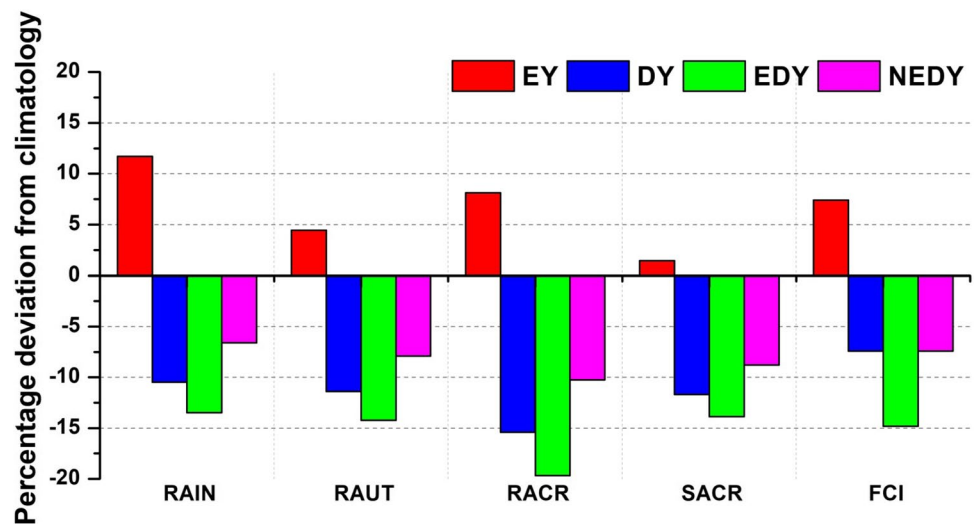

Fig. 4 Percentage deviation from the climatological values (averaged over central India: 72–88° E, 18–28° N) region) of the rainfall and different microphysical process for different composites (i.e., excess year (EY), El-Nino + deficient years (EDY), deficient years (DY), non-El-Nino + deficient years (NEDY)) considered in the study

summer, and nearly half of them are depressions (Godbole 1977; Mooley and Shukla 1987). These LPS move west-north-westward to dissipate the central Indian subcontinent

and rains maximum over the western part of LPS. This may be either due to a feedback mechanism between hydro-dynamic instabilities and cumulus heating in presence of

Fig. 5 Same as Fig. 2 but for the difference between active and break composites. The period is 1999–2008
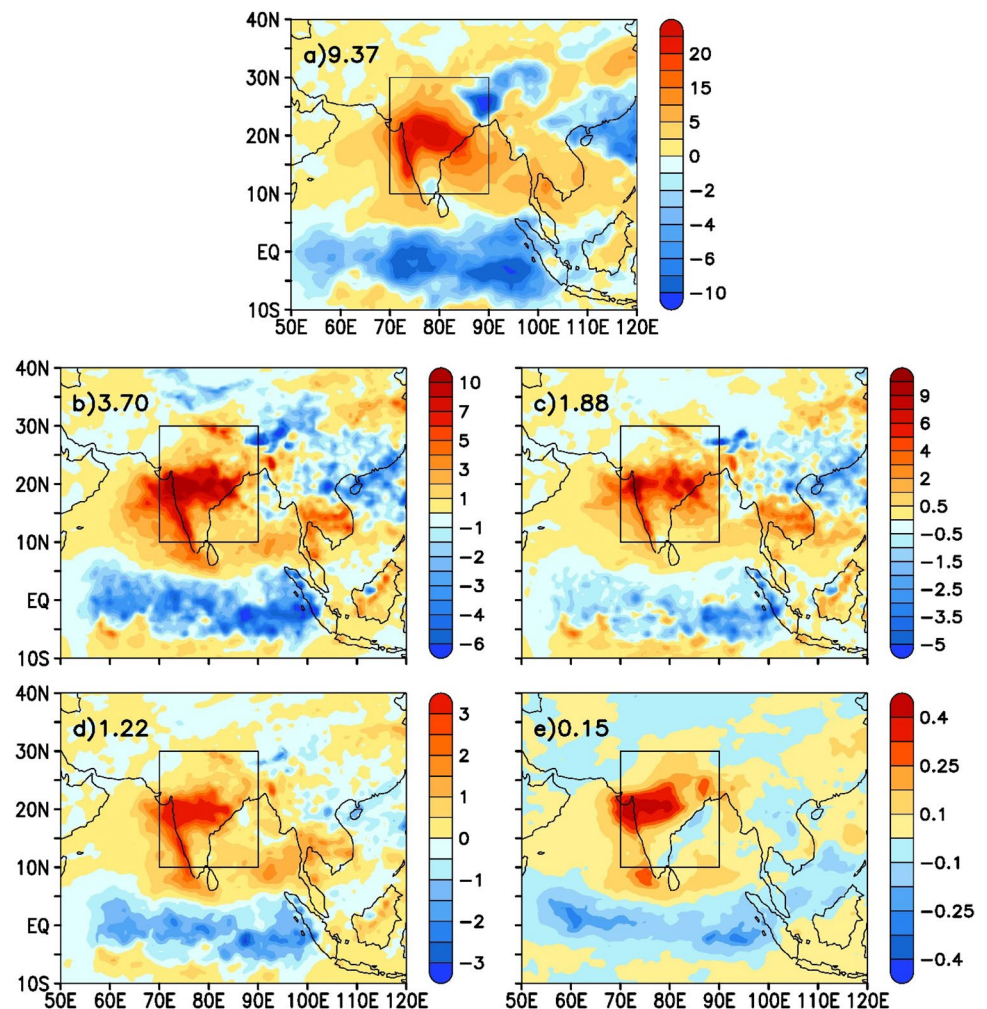
low-level vorticity and vertical velocity (Goswami 1987) or due to adiabatic nonlinear advection of potential vorticity maximum that consists the LPS (Boos et al. 2015). Here, we have studied the role of microphysical processes when these LPS pass through the central India region (Fig. 6). A total of 117 such LPS events originating from BoB and the Indian land area are analyzed here (Fig. S6). Out of these greatest number of LPS (84) are found to originate from BoB and there are 33 such events originating from the land area. Tracks of these events are prepared online using the Cyclone eAtlas-IMD (Fig. S6). We have also computed the composite of rainfall for these events during 1997–2019 only due to the availability of GPCP data. During LPS, more rain is observed over the ISM region (~ 9 mm/day, Fig. 6) compared to its climatological value (Fig. 1) of ~ 7.5 mm/day. The microphysical processes are also found to be strengthened during LPS. Stronger freezing of cloud ice (FCI) over BoB followed by the central India region (Fig. 6e) indicates the presence of deep convective clouds during LPS, which help to uplift more moisture below the freezing level to form cloud ice. Interestingly, the snow accretion process, which

is a process when ice crystals can collide with supercooled water droplets, is dominated over central India and the adjacent BoB region (Fig. 6d).

Now, we have computed the variance of microphysical processes, which in general can be done for rainfall to understand the vigor of convection in different temporal time scales (i.e., synoptic, 3–7 days; QBM, 10–20 days; and MISO, 30–60 days). The averaged sub-seasonal variance of microphysical processes in synoptic, QBM, and MISO scales is also shown in Fig. 7 (RAUT and RACR) and Fig. 8 (SACR and FCI). The variance of these processes is found to be more in the synoptic scale followed by QBM and MISO scale (Figs. 7 and 8). The high variance is noticed over central India and the equatorial Indian Ocean for all of these processes. The Western Ghats and northeast India also depict a high variance for RAUT, RACR, and SACR across all the sub-seasonal scales. We can see that the magnitude of variance is highest in rain autoconversion for each subseasonal scale compared to other microphysical processes. Since the microphysical processes differ significantly in their climatological mean value, the coefficient of variation (CV)

Fig. 6 Composite of rainfall and microphysical processes for the LPS events mentioned in the study. ISM region (70–90° E, 10–30° N) averaged value of respective variables are written at the top left corner. The central India region is shown in (**b**). Unit: mm/day
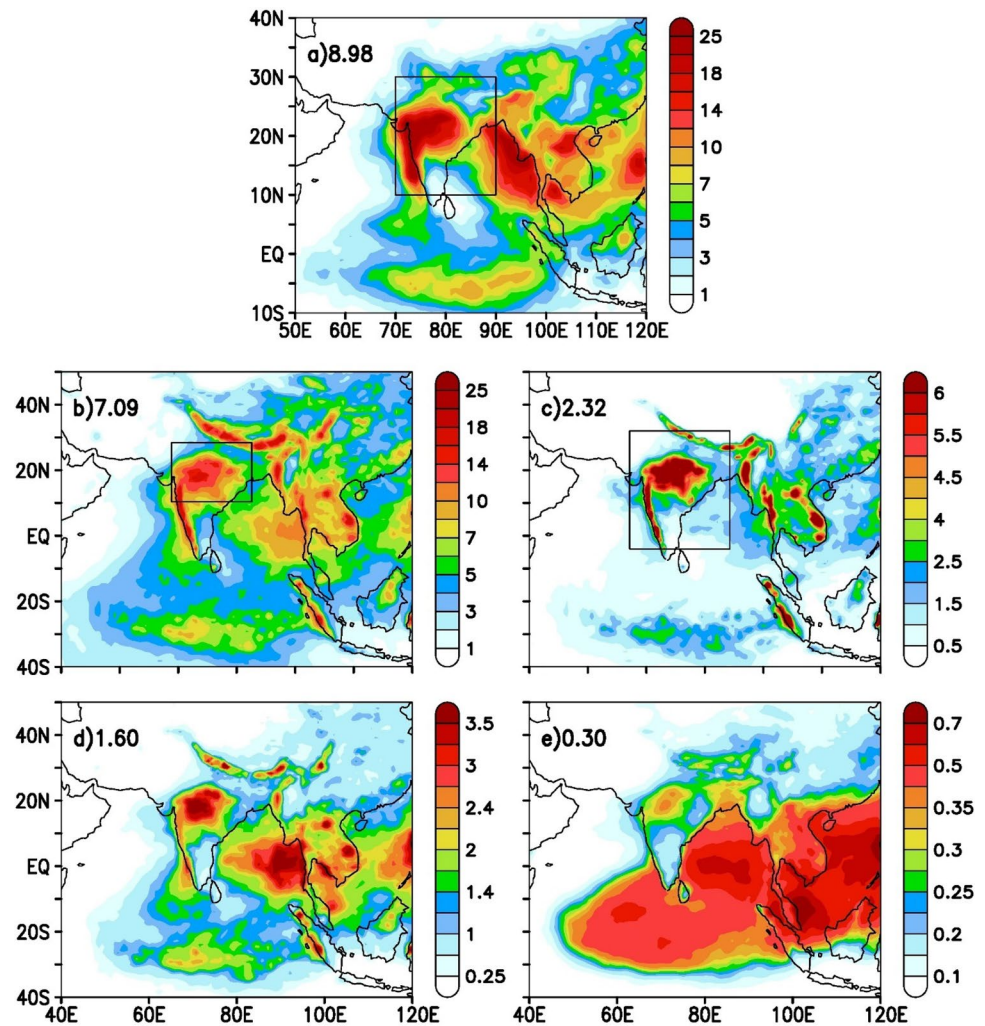

may be a better measure to compare the sub-seasonal variability of these processes. Table 1 contains the CV values of all the cloud microphysical processes averaged over the central India region. The CV is higher in the synoptic scale for all the cloud microphysical processes. The CV is the highest for RACR in all the sub-seasonal scales. The CV values gradually decrease from high frequency (Synoptic) to low frequency (QBM, MISO) for all the cloud microphysical processes.

To understand the relationship of microphysical processes on ISMR, we have computed the interannual correlation between sub-seasonal variances of each microphysical process (averaged over the ISM region) and mean ISMR (Fig. 9). The results reveal that synoptic variances of all these processes are more correlated with mean ISMR that QBM and MISO scales. For the synoptic case, FCI ($r \sim 0.7$) shows the highest correlation with mean ISMR, among all followed by SACR ($r \sim 0.65$), RACR ($r \sim 0.53$), and RAUT ($r \sim 0.45$), which will help for the targeted improvement in CGCMs. The high correlation of FCI and ISMR

in the synoptic scale is due to the formation of more cloud ice, snow, and graupel in presence of more moisture and stronger updrafts during lows and depressions. On the other hand, the correlation of FCI and ISMR decreases in the QBM scale ($r \sim 0.27$) and turns negative in the MISO scale ($r \sim -0.07$). This highlights the role of ice processes in the synoptic scale (e.g., lows and depression), where deep convective cloud dominates. The RAUT is also less significant in QBM ($r \sim 0.27$) and MISO ($r \sim 0.14$) scales. In the QBM scale, correlations of RACR ($r \sim 0.45$) and SACR ($r \sim 0.41$) with ISMR are only above the 95% significance level. In the MISO scale, only RACR ($r \sim 0.36$) is significantly correlated with ISMR. However, low correlation coefficient (CC) values of the MISO scale variance of the other processes with mean ISMR do not imply that they have low contribution to the mean ISMR. In principle, the MISO scale consists of active and break spells. Extended active (break) increases (decreases) the mean ISMR, but their variance is positive, which may result in low CC values (Saha et al. 2020) when combined.

Fig. 7 Variances of the RAUT and RACR in different sub-seasonal scales. Unit: mm²/day.²
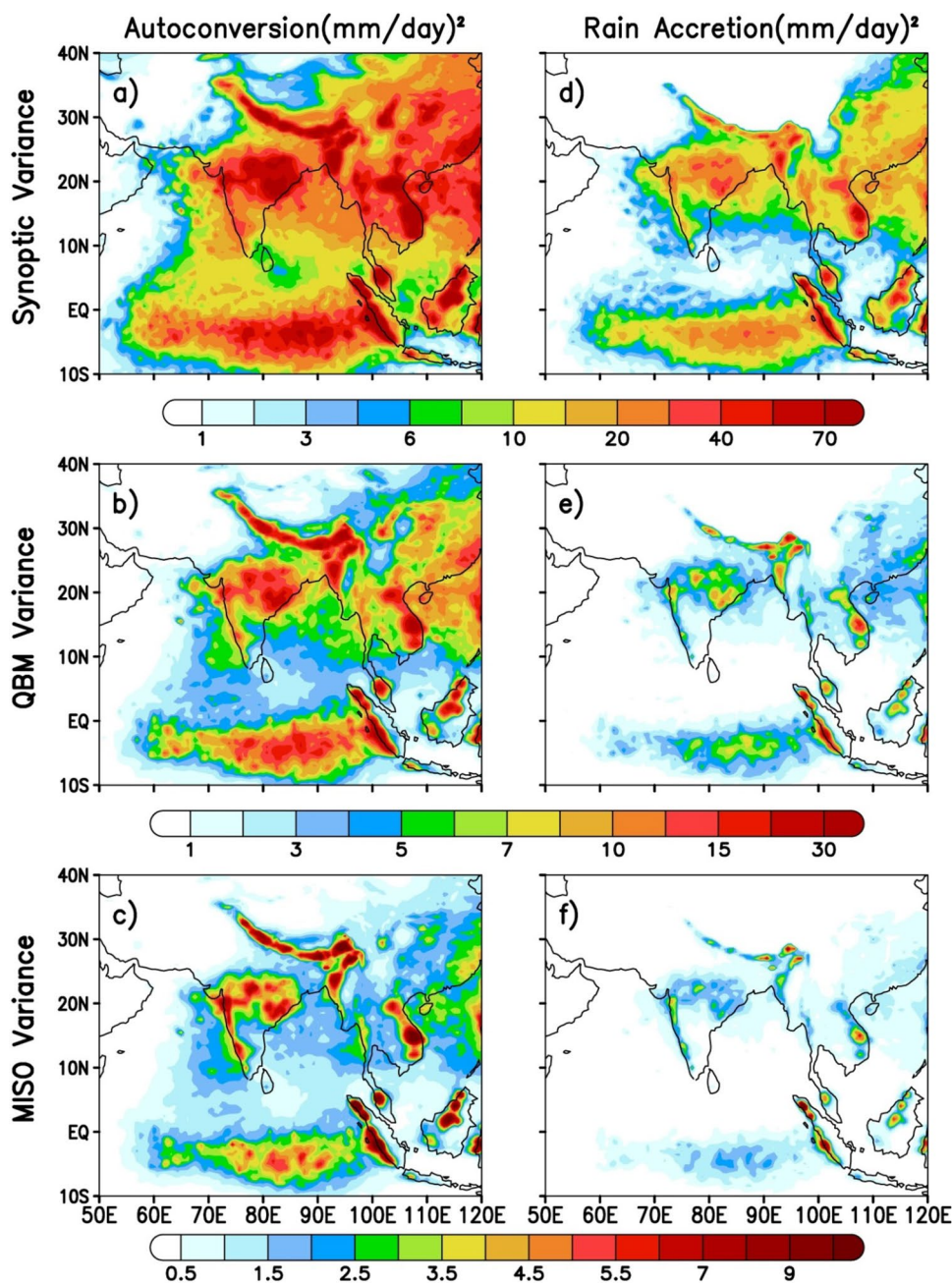
In recent studies, Saha et al. (2019, 2020, and 2021) also demonstrated an interesting relationship between the sub-seasonal variance of rainfall and mean ISMR across all periods. To find a similar relationship of the sub-seasonal variance of microphysical processes, with the mean ISMR, we have adapted the methodology from Saha et al.'s (2019) study. The methodology is briefly described as follows. Each microphysical process is spatially averaged (land region only) over central India (72° E–88° E, 18° N–28° N). This yields daily time series (40 years; 1980–2019) of the microphysical process for central India. Then, we calculated the time series (for each harmonic) after filtering out (low pass filter) the

harmonics up to 150th (i.e., 365/150 = 2.43 days of periodicity) each microphysical process one by one by Fourier analysis. The first four harmonics (i.e., 0, 1, 2, and 3) together represent the annual cycle. The remaining harmonics together represent the total anomaly of periodicity 2 − 91.25-day band (in a 365-day calendar year, the fifth harmonics represents 365/4 = 91.25 days of periodicity). One by one, harmonics are removed up to 150 (corresponds to 365/150 = 2.43 days) and reconstructed back into the time series of daily rainfall anomalies. Therefore, for each year, there will be 147-time series (i.e., an anomaly with harmonics greater than 3, 4, 5 … 150 corresponds to the anomaly of 2 − 91.25-, 2 − 75- …

Fig. 8 Same as Fig. 7 but for SACR and FCI
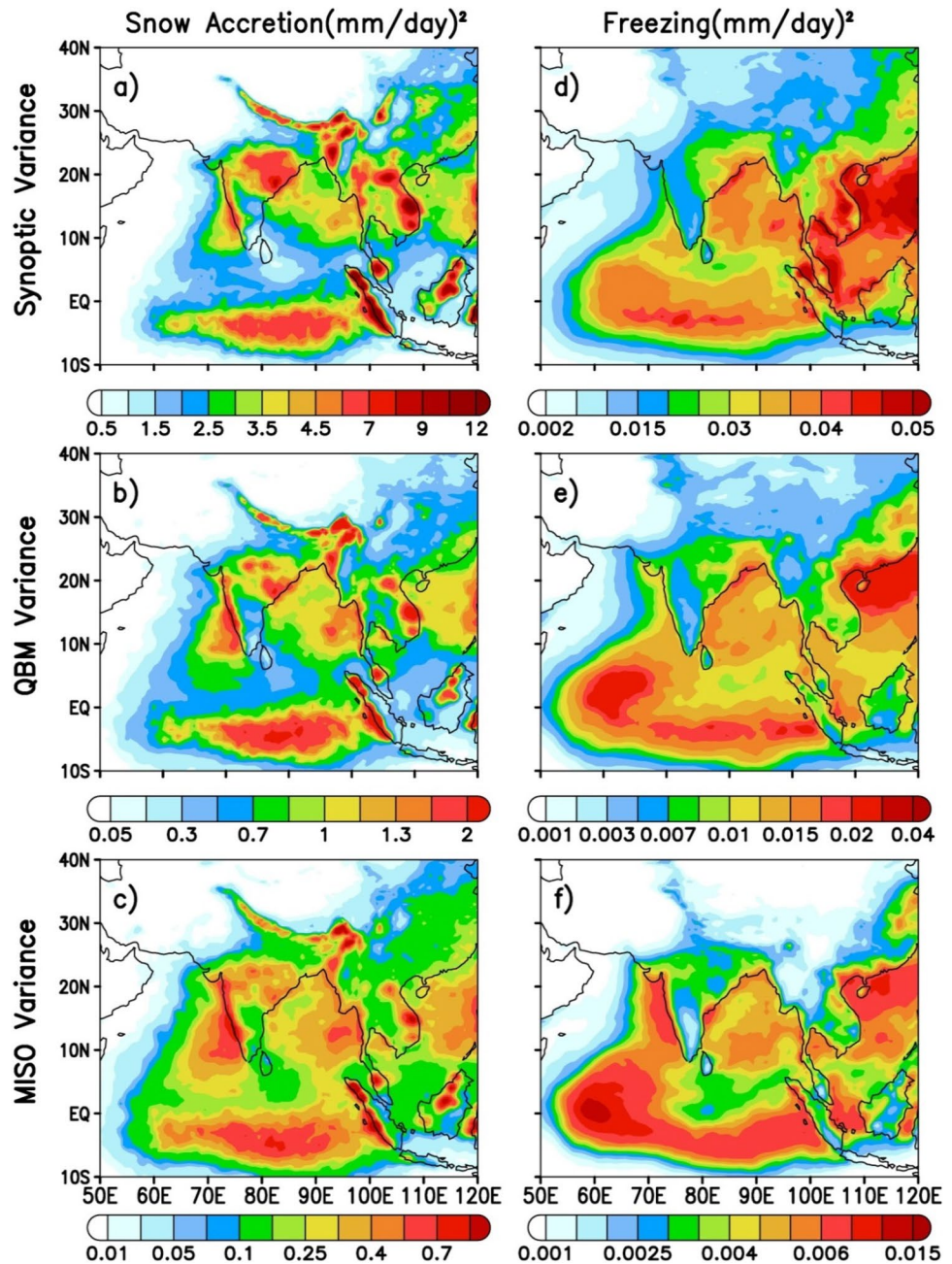
2−2.43-day bands respectively). Then, the seasonal (JJAS) variance of each filtered time series (i.e., 147 time series) is calculated and the same is correlated with the seasonal (JJAS)

Table 1 Coefficient of variation of cloud microphysical processes averaged over central India

Band	RAUT	RACR	SACR	FCI
Synoptic	1.00	1.77	1.35	0.56
QBM	0.50	0.87	0.68	0.34
MISO	0.28	0.48	0.37	0.21

mean of ISMR (70° E − 90°E, 10° N − 30° N, the land region only). Further, this variance is also correlated with mean Nino 3.4 SST to find the remote influence of ENSO (Fig. 10). Here, a specific period contains the oscillations of all periods less than 2 days. For example, period 10 stands for periodicity 2 − 10 and so on. The results reveal that, all of these processes show a significant and strong correlation in high-frequency scales (i.e., synoptic). The correlation falls rapidly at higher order periods and becomes less than 95% significant at around period 15 for RAUT and RACR. However, SACR and FCI become less significant after period ∼ 30. Among all the processes, FCI shows a peak at period ∼ 3. It also shows a strong
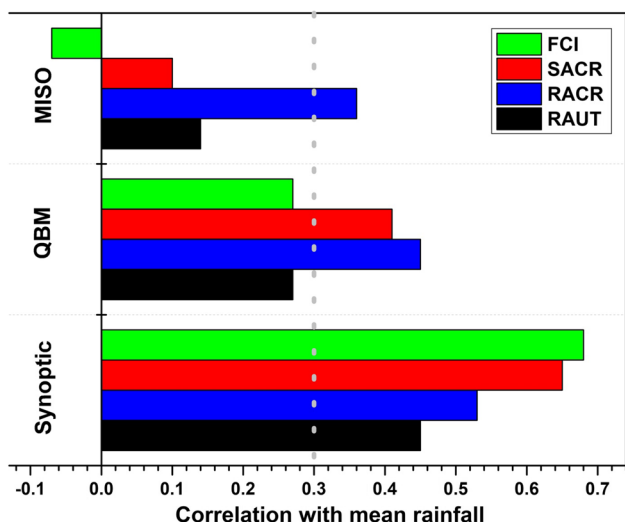
Fig. 9 Correlation between June to September (JJAS) variance of the microphysical process and the mean rainfall averaged over the ISM region
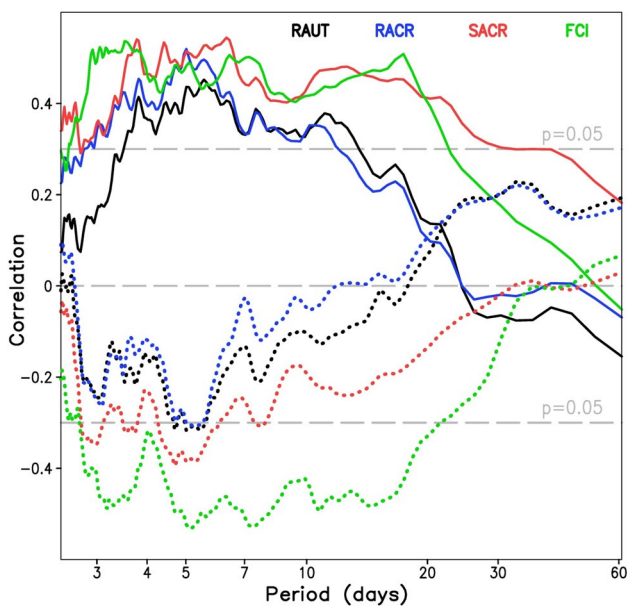
Fig. 10 Correlation of the seasonal (June to September average) mean ISMR (Niño3.4 SST) with the cumulative variance of different microphysical processes at various time bands (or period, i.e., 2.4–60 days) are shown in solid (dotted) lines. A significant correlation of 95% ($p = 0.05$) is also shown

association with Nino 3.4 SST at that period. FCI also holds a strong and significant correlation with Nino 3.4 SST up to period ~ 20. The other processes also show similar associations; however, their strength is less and mostly below the 95% significance level. All these results pinpoint the importance of microphysical processes in the synoptic scale to contribute to the seasonal mean ISMR.

3.4 Possible factors behind the interannual variability of cloud microphysical processes

Several studies (Dutta et al. 2020, 2021; Hazra et al. 2017a, b) have highlighted the importance of thermodynamical and dynamical factors behind the cloud microphysical processes. For this purpose, we have evaluated OLR (i.e., proxy of convection), mid-tropospheric specific humidity (i.e. availability of moisture, Fletcher et al. 2020), high cloud fractions (HCF), and lower tropospheric circulation (850 hPa). The mean value of OLR (averaged over the Bay of Bengal., $80 - 100°$ E, $10 - 20°$ N), SH, and HCF averaged over the ISM region are shown in Fig. 11 for different composites (NY, EY, DY, EDY, and NEDY). High (low) values of OLR represent shallow (deep) convection. A decrease in OLR (~ 1 W/m^2) is noticed in EY (203.6 W/m^2) from NY (204.7 W/m^2). Drought years are associated with significantly less convection (i.e., more OLR, 206.4 W/m^2). A significant difference between EY and DY is also noticed for SH (~ 0.4 g/kg) and HCF (~ 7%). During EDY (OLR ~ 207 W/m^2), the convection is even less than that of NEDY (OLR ~ 205 W/m^2) which is consistent with SH and HCF. The low-level jet (850 hPa, averaged over $50 - 65°$ E, $5 - 15°$ N) is also found to be stronger in EY than that DY (Fig. 12). Its strength is less in EDY than NEDY. The Indian monsoon circulation is characterized by a strong low-level southwesterly jet (Findlater jet), which peaks around the Somali coast and Arabian Sea region. This low-level jet (LLJ) connects the Mascarene high and Indian monsoon trough and forms the lower branch of the monsoon Hadley cell. The stronger (weaker) LLJ during indicates more (less) influx of moisture (Wilson et al. 2018) over the Indian region which is responsible for excess (deficient) monsoon. De et al. (2016) also showed that the proper modulation of the LLJ over the oceanic region, during a deficient monsoon event, is manifested through the weak eastward moisture flux. The availability of moisture plays a significant role in controlling the cloud microphysical processes (Hazra et al. 2016). The LLJ over the Indian ocean is weakened during El-Nino (Wilson et al. 2018) which is also responsible for warmer SST anomalies over the western Indian Ocean. Babu and Joseph (2002) also found that warmer SST anomalies over the north Indian ocean are found during EDY than NEDY.

4 Conclusions

The present study illustrates the budget of detailed microphysical processes (tendency terms or production rates) from the GEOS model (MERRA2 reanalysis) during extreme monsoon years. The variance (represent the vigorous fluctuations) of microphysical processes in the different temporal domain (e.g., synoptic, QBM, MISO) and in relation

Fig. 11 High cloud fraction and mid-tropospheric (300–700 hPa) specific humidity averaged over the ISM region are shown in black and red lines. OLR averaged over the Bay of Bengal region is shown in blue line for normal year (NY), excess year (EY), El-Nino + deficient years (EDY), deficient years (DY), non-El-Nino + deficient years (NEDY)
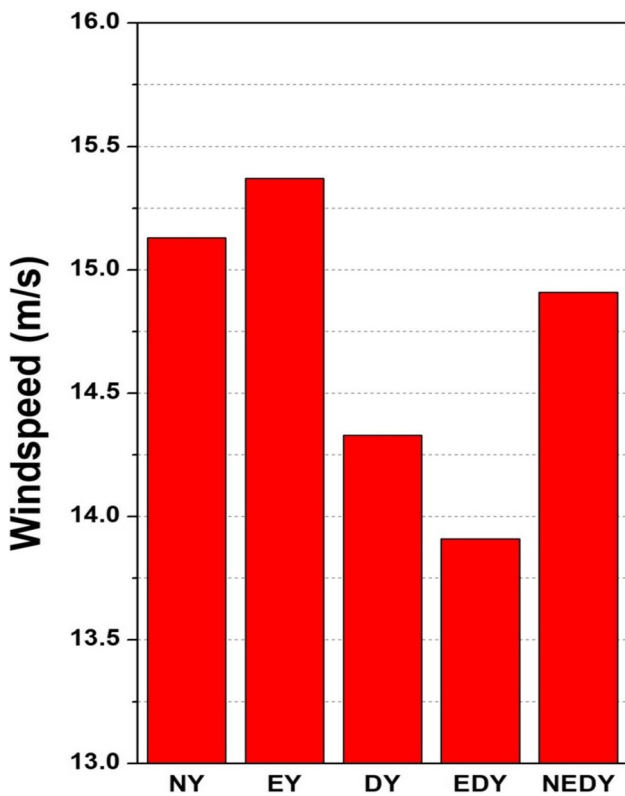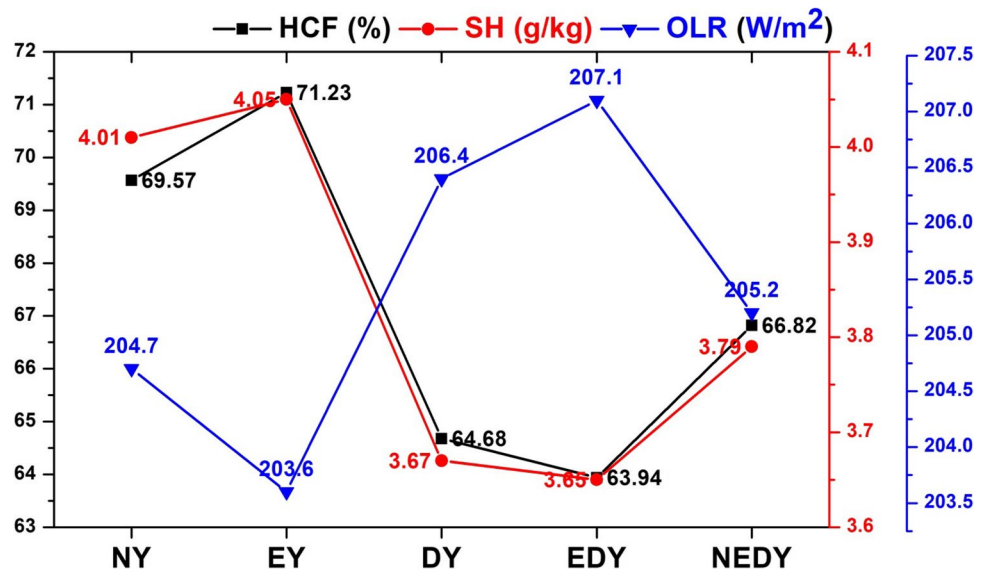

Fig. 12 Lower tropospheric circulation (850 hPa) averaged over Box (50–65° E, 5–15° N) for different composites (normal year (NY), excess year (EY), El-Nino + deficient years (EDY), deficient years (DY), non-El-Nino + deficient years (NEDY))

to ISMR is also demonstrated in this present work, which is important for interannual variability and the seasonal mean. The understanding based on the results analyzed here indicates the pathways to improve the shortcomings

in the CGCMs. In this study, we have discussed the role of these microphysical processes behind the ISMR in interannual and sub-seasonal scales. The major findings are summarized below:

i)   The microphysical processes are well associated with the seasonal mean rainfall and play a significant role in the interannual variability of the monsoon. During excess (deficient) years they increase (decrease) significantly.

ii)   The microphysical processes are found to be linked with large-scale phenomena i.e., ENSO. The difference in composites between EDY and NEDY demonstrates that during deficient years accompanied with El-Nino, these processes are weakened even more.

iii)   These microphysical processes are strengthened during active spells as compared to break spells and also have significant sub-seasonal variability. The variance is more in the synoptic scale compared to QBM and MISO.

iv)   The sub-seasonal variances of the microphysical processes are well correlated with the mean rainfall. Correlation is stronger in the synoptic scale. The synoptic scale variances of these processes are also well correlated with Nino 3.4 SST which may imply the remote influence of ENSO on them. When the LPS moves through the central India region, all these microphysical processes increase significantly.

This study concludes that, microphysical processes play a seminal role in governing the interannual and sub-seasonal variation of rainfall, backed by thermodynamical and dynamical features. Therefore, revisiting the processes in the microphysical scheme of the global climate model and targeted modification to improve the particular processes

will help to progress ISMR simulation from sub-seasonal to seasonal time scale.

Declarations

References

Adler RF, Huffman GJ, Chang A et al (2003) The version-2 global precipitation climatology project (GPCP) monthly precipitation analysis (1979-present). J Hydrometeorol 4:1147–1167. https://doi.org/10.1175/1525-7541(2003)004%3c1147:TVGPCP%3e2.0.CO;2

Babu CA, Joseph PV (2002) Post-monsoon sea surface temperature and convection anomalies over Indian and Pacific oceans. Int J Climatol 22:559–567. https://doi.org/10.1002/joc.729

Bacmeister JT, Suarez MJ, Robertson FR (2006) Rain reevaporation, boundary layer-convection interactions, and pacific rainfall patterns in an AGCM. J Atmos Sci 63:3383–3403. https://doi.org/10.1175/JAS3791.1

Bao X, Zhang F (2019) How accurate are modern atmospheric reanalyses for the data-sparse tibetan plateau region? J Clim 32:7153–7172. https://doi.org/10.1175/JCLI-D-18-0705.1

Barahona D, Molod A, Bacmeister J et al (2014) Development of two-moment cloud microphysics for liquid and ice within the NASA Goddard Earth Observing System Model (GEOS-5). Geosci Model Dev 7:1733–1766. https://doi.org/10.5194/gmd-7-1733-2014

Boos WR, Hurley JV, Murthy VS (2015) Adiabatic westward drift of Indian monsoon depressions. Q J R Meteorol Soc 141:1035–1048. https://doi.org/10.1002/qj.2454

Borah PJ, Venugopal V, Sukhatme J et al (2020) Indian monsoon derailed by a North Atlantic wavetrain. Science 80(370):1335–1338. https://doi.org/10.1126/science.aay6043

Burns SJ, Fleitmann D, Matter A et al (2003) Indian Ocean climate and an absolute chronology over Dansgaard/Oeschger events 9 to 13. Science 80(301):1365–1367. https://doi.org/10.1126/science.1086227

Chakravarty K, Pokhrel S, Kalshetti M et al (2018) Unraveling of cloud types during phases of monsoon intra-seasonal oscillations by a Ka-band Doppler weather radar. Atmos Sci Lett 19:e847. https://doi.org/10.1002/asl.847

Chang CP, Harr P, Ju J (2001) Possible roles of atlantic circulation on the weakening Indian monsoon rainfall-ENSO relationship. J Clim 14:2376–2380. https://doi.org/10.1175/1520-0442(2001)014%3c2376:PROACO%3e2.0.CO;2

Chattopadhyay R, Phani R, Sabeerali CT et al (2015) Influence of extratropical sea-surface temperature on the Indian summer monsoon: an unexplored source of seasonal predictability. Q J R Meteorol Soc 141:2760–2775. https://doi.org/10.1002/qj.2562

Cheng CT, Wang WC, Chen JP (2007) A modelling study of aerosol impacts on cloud microphysics and radiative properties. Q J R Meteorol Soc 133:283–297. https://doi.org/10.1002/qj.25

Choudhury BA, Rajesh PV, Zahan Y, Goswami BN (2021) Evolution of the Indian summer monsoon rainfall simulations from CMIP3 to CMIP6 models. Clim Dyn 58:2637–2662. https://doi.org/10.1007/s00382-021-06023-0

De S, Hazra A, Chaudhari HS (2016) Does the modification in "critical relative humidity" of NCEP CFSv2 dictate Indian mean summer monsoon forecast? Evaluation through thermodynamical and dynamical aspects. Clim Dyn 46:1197–1222. https://doi.org/10.1007/s00382-015-2640-z

De S, Agarwal NK, Hazra A et al (2019) On unravelling mechanism of interplay between cloud and large scale circulation: a grey area in climate science. Clim Dyn 52:1547–1568. https://doi.org/10.1007/s00382-018-4211-6

Dutta U, Chaudhari HS, Hazra A et al (2020) Role of convective and microphysical processes on the simulation of monsoon intraseasonal oscillation. Clim Dyn 55:2377–2403. https://doi.org/10.1007/s00382-020-05387-z

Dutta U, Hazra A, Chaudhari HS et al (2021) Role of microphysics and convective autoconversion for the better simulation of tropical intraseasonal oscillations (MISO and MJO). J Adv Model Earth Syst 13:e2021MS002540. https://doi.org/10.1029/2021ms002540

Dutta U, Hazra A, Chaudhari HS, Saha SK, Pokhrel S, Verma U (2022) Unraveling the global teleconnections of Indian summer monsoon clouds: expedition from CMIP5 to CMIP6. Global Planet Change 215:103873. https://doi.org/10.1016/j.gloplacha.2022.103873,1-12

Dwivedi S, Goswami BN, Kucharski F (2015) Unraveling the missing link of ENSO control over the Indian monsoon rainfall. Geophys Res Lett 42:8201–8207. https://doi.org/10.1002/2015GL065909

Fletcher JK, Parker DJ, Turner AG et al (2020) The dynamic and thermodynamic structure of the monsoon over southern India: New observations from the INCOMPASS IOP. Q J R Meteorol Soc 146:2867–2890. https://doi.org/10.1002/qj.3439

Gadgil S, Gadgil S (2006) The Indian monsoon, GDP and agriculture. Econ Polit Wkly 41 (47):4887–4895

Gelaro R, McCarty W, Suárez MJ et al (2017) The modern-era retrospective analysis for research and applications, version 2 (MERRA-2). J Clim 30:5419–5454. https://doi.org/10.1175/JCLI-D-16-0758.1

Godbole RV (1977) The composite structure of the monsoon depression. Tellus 29:25–40. https://doi.org/10.3402/tellusa.v29i1.11327

Goswami BN (1987) A mechanism for the west-north-west movement of monsoon depressions. Nature 326:376–378. https://doi.org/10.1038/326376a0

Goswami BN (2005) South Asian monsoon. In: Intraseasonal variability in the atmosphere-ocean climate system. Springer Praxis Books (Environmental Sciences). Springer, Berlin, Heidelberg. https://doi.org/10.1007/3-540-27250-X_2

Goswami BB, Goswami BN (2017) A road map for improving dry-bias in simulating the South Asian monsoon precipitation by climate models. Clim Dyn 49:2025–2034. https://doi.org/10.1007/s00382-016-3439-2

Goswami BN, Jayavelu V (2001) On possible impact of the Indian summer monsoon on the ENSO. Geophys Res Lett 28:571–574. https://doi.org/10.1029/2000GL011485

Goswami BN, Xavier PK (2005) ENSO control on the south Asian monsoon through the length of the rainy season. Geophys Res Lett 32:1–4. https://doi.org/10.1029/2005GL023216

Goswami BN, Ajayamohan RS, Xavier PK, Sengupta D (2003) Clustering of low-pressure systems during the Indian summer monsoon by intraseasonal oscillations. Geophys Res Lett 30(8):1431. https://doi.org/10.1029/2002GL016734

Grabowski WW (1998) Toward cloud resolving modeling of large-scale tropical circulations: a simple cloud microphysics parameterization. J Atmos Sci 55:3283–3298. https://doi.org/10.1175/1520-0469(1998)055%3c3283:TCRMOL%3e2.0.CO;2

Hamal K, Sharma S, Khadka N et al (2020) Evaluation of MERRA-2 precipitation products using gauge observation in Nepal. Hydrology 7:1–21. https://doi.org/10.3390/hydrology7030040

Hazra A, Goswami BN, Chen J-P (2013) Role of interactions between aerosol radiative effect, dynamics, and cloud microphysics on transitions of monsoon intraseasonal oscillations. J Atmos Sci 70:2073–2087. https://doi.org/10.1175/JAS-D-12-0179.1

Hazra A, Chaudhari HS, Pokhrel S, Saha SK (2016) Indian summer monsoon precipitating clouds: role of microphysical process rates. Clim Dyn 46:2551–2571. https://doi.org/10.1007/s00382-015-2717-8

Hazra A, Chaudhari HS, Rao SA et al (2015) Impact of revised cloud microphysical scheme in CFSv2 on the simulation of the Indian summer monsoon. Int J Climatol 35:4738–4755. https://doi.org/10.1002/joc.4320

Hazra A, Chaudhari HS, Saha SK et al (2017a) Progress towards achieving the challenge of Indian summer monsoon climate simulation in a coupled ocean-atmosphere model. J Adv Model Earth Syst 9:2268–2290. https://doi.org/10.1002/2017MS000966

Hazra A, Chaudhari HS, Saha SK, Pokhrel S (2017b) Effect of cloud microphysics on Indian summer monsoon precipitating clouds: a coupled climate modeling study. J Geophys Res 122:3786–3805. https://doi.org/10.1002/2016JD026106

Hazra A, Chaudhari HS, Saha Subodh K, Pokhrel S, Dutta U, Goswami BN (2020a) Role of cloud microphysics in improved simulation of the Asian monsoon quasi-biweekly mode (QBM), Clim Dyn 54: 599–614. https://doi.org/10.1007/s00382-019-05015-5

Hazra V, Pattnaik S, Sisodiya A et al (2020b) Assessing the performance of cloud microphysical parameterization over the Indian region: simulation of monsoon depressions and validation with INCOMPASS observations. Atmos Res 239:104925. https://doi.org/10.1016/j.atmosres.2020.104925

Hendricks WA, Robey KW (1936) The sampling distribution of the coefficient of variation. Ann Math Stat 7:129–132. https://doi.org/10.1214/aoms/1177732503

Hersbach H, Bell B, Berrisford P et al (2020) The ERA5 global reanalysis. Q J R Meteorol Soc 146:1999–2049. https://doi.org/10.1002/qj.3803

Hunt KMR, Turner AG, Inness PM et al (2016) On the structure and dynamics of Indian monsoon depressions. Mon Weather Rev 144:3391–3416. https://doi.org/10.1175/MWR-D-15-0138.1

Hurley JV, Boos WR (2015) A global climatology of monsoon low-pressure systems. Q J R Meteorol Soc 141:1049–1064. https://doi.org/10.1002/qj.2447

Jones E, Wing AA, Parfitt R (2021) A global perspective of tropical cyclone precipitation in reanalyses. J Clim 34:8461–8480. https://doi.org/10.1175/JCLI-D-20-0892.1

Kessler E (1969) On the distribution and continuity of water substance in atmospheric circulations. In: On the distribution and continuity of water substance in atmospheric circulations. Meteorol Monogr 10(32):84

Khairoutdinov M, Kogan Y (2000) A new cloud physics parameterization in a large-eddy simulation model of marine stratocumulus. Mon Weather Rev 128:229–243. https://doi.org/10.1175/1520-0493(2000)128%3c0229:ANCPPI%3e2.0.CO;2

Kleist DT, Parrish DF, Derber JC et al (2009) Introduction of the GSI into the NCEP global data assimilation system. Weather Forecast 24:1691–1705. https://doi.org/10.1175/2009WAF2222201.1

Krishna Kumar K, Hoerling M, Rajagopalan B (2005) Advancing dynamical prediction of Indian monsoon rainfall. Geophys Res Lett 32:1–4. https://doi.org/10.1029/2004GL021979

Krishnamurthy V, Ajayamohan RS (2010) Composite structure of monsoon low pressure systems and its relation to Indian rainfall. J Clim 23:4285–4305. https://doi.org/10.1175/2010JCLI2953.1

Krishnamurthy V, Goswami BN (2000) Indian monsoon-ENSO relationship on interdecadal timescale. J Clim 13:579–595. https://doi.org/10.1175/1520-0442(2000)013%3c0579:IMEROI%3e2.0.CO;2

Kulkarni A, Kripalani R, Sabade S, Rajeevan M (2011) Role of intraseasonal oscillations in modulating Indian summer monsoon rainfall. Clim Dyn 36:1005–1021. https://doi.org/10.1007/s00382-010-0973-1

Kumar S, Arora A, Chattopadhyay R et al (2017) Seminal role of stratiform clouds in large-scale aggregation of tropical rain in boreal summer monsoon intraseasonal oscillations. Clim Dyn 48:999–1015. https://doi.org/10.1007/s00382-016-3124-5

Liebmann B, Smith CA (1996) Description of a complete (interpolated) outgoing longwave radiation dataset. Bull Am Meteor Soc 77:1275–1277

Liu Y, Daum PH, McGraw R (2004) An analytical expression for predicting the critical radius in the autoconversion parameterization. Geophys Res Lett 31:L06121. https://doi.org/10.1029/2003gl019117

Liu Y, Daum PH, McGraw RL (2005) Size truncation effect, threshold behavior, and a new type of autoconversion parameterization. Geophys Res Lett 32:1–5. https://doi.org/10.1029/2005GL022636

Luan L, Staten PW, Chi OAO, Qiang FU (2020) Seasonal and annual changes of the regional tropical belt in GPS-RO measurements and reanalysis datasets. J Clim 33:4083–4094. https://doi.org/10.1175/JCLI-D-19-0671.1

Mason BJ (1971) The physics of clouds. Oxford Univ. Press, Oxford, p 671

Meehl GA (1989) The coupled ocean—atmosphere modeling problem in the tropical Pacific and Asian monsoon regions. J Clim 2:1146–1163. https://doi.org/10.1175/1520-0442(1989)002%3c1146:tcompi%3e2.0.co;2

Molod A, Takacs L, Suarez M, Bacmeister J (2015) Development of the GEOS-5 atmospheric general circulation model: evolution from MERRA to MERRA2. Geosci Model Dev 8:1339–1356. https://doi.org/10.5194/gmd-8-1339-2015

Mooley DA, Parthasarathy B (1984) Fluctuations in All-India summer monsoon rainfall during 1871–1978. Clim Change 6:287–301. https://doi.org/10.1007/BF00142477

Mooley DA, Shukla J (1987) Variability and forecasting of the summer monsoon rainfall over India. In: Chang CP, Krishnamurti TN (eds) Monsoon meteorology. Oxford University Press, New York, pp 26–58

Moorthi S, Suarez MJ (1992) Relaxed Arakawa-Schubert: a parameterization of moist convection for general circulation models. Mon Weather Rev 120:978–1002. https://doi.org/10.1175/1520-0493(1992)120%3c0978:RASAPO%3e2.0.CO;2

Nobre P, Shukla J (1996) Variations of sea surface temperature, wind stress, and rainfall over the tropical Atlantic and South America. J Clim 9:2464–2479. https://doi.org/10.1175/1520-0442(1996)009%3c2464:VOSSTW%3e2.0.CO;2

Parthasarathy B, Diaz HF, Eischeid JK (1988) Prediction of all-India summer monsoon rainfall with regional and large-scale parameters. J Geophys Res 93:5341–5350. https://doi.org/10.1029/JD093iD05p05341

Pokhrel S, Chaudhari HS, Saha SK et al (2012) ENSO, IOD and Indian Summer Monsoon in NCEP climate forecast system. ClimDyn 39:2143–2165. https://doi.org/10.1007/s00382-012-1349-5

Pradhan PK, Prasanna V, Lee DY, Lee MI (2016) El Niño and Indian summer monsoon rainfall relationship in retrospective seasonal prediction runs: experiments with coupled global climate models and MMEs. Meteorol Atmos Phys 128:97–115. https://doi.org/10.1007/s00703-015-0396-y

Prasad K, Kalsi SR, Datta RK (1990) On some aspects of wind and cloud structure of monsoon depressions. Mausam (New Delhi) 41:365–370

Praveen V, Sandeep S, Ajayamohan RS (2015) On the relationship between mean monsoon precipitation and low pressure systems in climate model simulations. J Clim 28:5305–5324. https://doi.org/10.1175/JCLI-D-14-00415.1

Pruppacher HR, Klett JD (1997) Microphysics of clouds and precipitation, 2nd edn. Kluwer Academic, Dordrecht, p 954

Putman WM, Lin SJ (2007) Finite-volume transport on various cubed-sphere grids. J Comput Phys 227:55–78. https://doi.org/10.1016/j.jcp.2007.07.022

Rajeevan M, Rohini P, Niranjan Kumar K et al (2013) A study of vertical cloud structure of the Indian summer monsoon using CloudSat data. Clim Dyn 40:637–650. https://doi.org/10.1007/s00382-012-1374-4

Rajeevan M, Unnikrishnan CK, Preethi B (2012) Evaluation of the ENSEMBLES multi-model seasonal forecasts of Indian summer monsoon variability. ClimDyn 38:2257–2274. https://doi.org/10.1007/s00382-011-1061-x

Rayner NA, Parker DE, Horton EB, Folland CK, Alexander LV, Rowell DP et al (2003) Global analyses of sea surface temperature, sea ice, and night marine air temperature since the late nineteenth century. J Geophys Res Atmos 108(D14):447. https://doi.org/10.1029/2002jd002670

Reichle RH, Draper CS, Liu Q et al (2017) Assessment of MERRA-2 land surface hydrology estimates. J Clim 30:2937–2960. https://doi.org/10.1175/JCLI-D-16-0720.1

Revadekar JV, Varikoden H, Preethi B, Mujumdar M (2016) Precipitation extremes during Indian summer monsoon: role of cyclonic disturbances. Nat Hazards 81:1611–1625. https://doi.org/10.1007/s11069-016-2148-9

Rienecker MM, Coauthors (2008) The GEOS-5 data assimilation system—documentation of versions 5.0.1 and 5.1.0, and 5.2.0. NASA Tech Rep Ser Glob Model Data Assim, Editor Max J. Suarez, NASA/TM-2008–104606, Vol. 27:1–118

Ropelewski CF, Halpert MS (1989) Precipitation patterns associated with the high index phase of the Southern Oscillation. J Clim 2:268–284. https://doi.org/10.1175/1520-0442(1989)002%3c0268:ppawth%3e2.0.co;2

Saha SK, Hazra A, Pokhrel S et al (2019) Unraveling the mystery of Indian summer monsoon prediction: improved estimate of predictability limit. J Geophys Res Atmos 124:1962–1974. https://doi.org/10.1029/2018JD030082

Saha SK, Hazra A, Pokhrel S et al (2020) Reply to Comment by E. T. Swenson, D. Das, and J. Shukla on "Unraveling the mystery of Indian summer monsoon prediction: improved estimate of predictability limit." J Geophys Res Atmos 125:e2020JD033242. https://doi.org/10.1029/2020JD033242

Saha SK, Konwar M, Pokhrel S et al (2021) Interplay between subseasonal rainfall and global predictors in modulating interannual to multidecadal predictability of the ISMR. Geophys Res Lett 48:e2020GL091458. https://doi.org/10.1029/2020GL091458

Sankar S, Svendsen L, Gokulapalan B et al (2016) The relationship between Indian summer monsoon rainfall and Atlantic multidecadal variability over the last 500 years. Tellus, Ser A Dyn Meteorol Oceanogr 68(1):31717. https://doi.org/10.3402/tellusa.v68.31717

Sarker RP, Choudhary A (1988) A diagnostic study of monsoon depressions. Mausam (New Delhi) 39:9–18

Sikka DR (1980) Some aspects of the large scale fluctuations of summer monsoon rainfall over India in relation to fluctuations in the planetary and regional scale circulation parameters. Proc Indian Acad Sci Earth Planet Sci 89:179–195. https://doi.org/10.1007/BF02913749

Sikka DR, Gadgil S (1980) On the maximum cloud zone and the ITCZ over Indian longitudes during the southwest monsoon. Mon Weather Rev 108:1840–1853. https://doi.org/10.1175/1520-0493(1980)108%3c1840:OTMCZA%3e2.0.CO;2

Srivastava AK, Rajeevan M, Kulkarni R (2002) Teleconnection of OLR and SST anomalies over Atlantic Ocean with Indian summer monsoon. Geophys Res Lett 29(8):1284. https://doi.org/10.1029/2001GL013837

Stano G, Krishnamurti TN, Vijaya Kumar TSV, Chakraborty A (2002) Hydrometeor structure of a composite monsoon depression using the TRMM radar. Tellus A Dyn Meteorol Oceanogr 54:370–381. https://doi.org/10.3402/tellusa.v54i4.12154

Stowasser M, Annamalai H, Hafner J (2009) Response of the South Asian summer monsoon to global warming: mean and synoptic systems. J Clim 22:1014–1036. https://doi.org/10.1175/2008JCLI2218.1

Tao WK, Simpson J, Lang S et al (1990) An algorithm to estimate the heating budget from vertical hydrometeor profiles. J Appl Meteorol 29:1232–1244. https://doi.org/10.1175/1520-0450(1990)029%3c1232:aateth%3e2.0.co;2

Tao WK, Lang S, Olson WS et al (2001) Retrieved vertical profiles of latent heat release using TRMM rainfall products for February 1988. J Appl Meteorol 40:957–982. https://doi.org/10.1175/1520-0450(2001)040%3c0957:RVPOLH%3e2.0.CO;2

Tiwari PR, Kar SC, Mohanty UC et al (2014) Skill of precipitation prediction with GCMs over north India during winter season. Int J Climatol 34:3440–3455. https://doi.org/10.1002/joc.3921

Trenberth KE, Stepaniak DP, Caron JM (2000) The global monsoon as seen through the divergent atmospheric circulation. J Clim 13:3969–3993. https://doi.org/10.1175/1520-0442(2000)013%3c3969:TGMAST%3e2.0.CO;2

Tripoli GJ, Cotton WR (1980) A numerical investigation of several factors contributing to the observed variable intensity of deep convection over South Florida. J Appl Meteorol 19:1037–1063. https://doi.org/10.1175/1520-0450(1980)019%3c1037:ANIOSF%3e2.0.CO;2

Wang B, Ding Q, Fu X et al (2005) Fundamental challenge in simulation and prediction of summer monsoon rainfall. Geophys Res Lett 32: L15711. https://doi.org/10.1029/2005GL022734

Wilson SS, Joseph PV, Mohanakumar K, Johannessen OM (2018) Interannual and long term variability of low level jetstream of the Asian summer monsoon. Tellus, Ser A Dyn Meteorol Oceanogr 70(1):1–9. https://doi.org/10.1080/16000870.2018.1445380

Wonsick MM, Pinker RT, Govaerts Y (2009) Cloud variability over the Indian monsoon region as observed from satellites. J Appl Meteorol Climatol 48:1803–1821. https://doi.org/10.1175/2009JAMC2027.1

Wood R (2005) Drizzle in stratiform boundary layer clouds. Part II: Microphysical aspects. J Atmos Sci 62:3034–3050. https://doi.org/10.1175/JAS3530.1

Wu P, Xi B, Dong X, Zhang Z (2018) Evaluation of autoconversion and accretion enhancement factors in general circulation model warm-rain parameterizations using ground-based measurements over the Azores. Atmos Chem Phys 18:17405–17420. https://doi.org/10.5194/acp-18-17405-2018

Wu WS, Purser RJ, Parrish DF (2002) Three-dimensional variational analysis with spatially inhomogeneous covariances. Mon Weather Rev 130:2905–2916. https://doi.org/10.1175/1520-0493(2002)130%3c2905:TDVAWS%3e2.0.CO;2

Yamasaki M (2013) A study on the effects of the ice microphysics on tropical cyclones. Adv Meteorol 2013:573786. https://doi.org/10.1155/2013/573786

Zhao Q, Carr FH (1997) A prognostic cloud scheme for operational NWP models. Mon Weather Rev 125:1931–1953. https://doi.org/10.1175/1520-0493(1997)125%3c1931:APCSFO%3e2.0.CO;2

Zhao X, Lin Y, Peng Y et al (2017) A single ice approach using varying ice particle properties in global climate model microphysics. J Adv Model Earth Syst 9:2138–2157. https://doi.org/10.1002/2017MS000952

Zhou T, Yu R, Li H, Wang B (2008) Ocean forcing to changes in global monsoon precipitation over the recent half-century. J Clim 21:3833–3852. https://doi.org/10.1175/2008JCLI2067.1